

PROSPECTS FOR RADIOWAVE
AND ACOUSTIC DETECTION
OF ULTRA- AND SUPERHIGH ENERGY
COSMIC NEUTRINOS (CROSS SECTIONS,
SIGNALS, THRESHOLDS)

*A.V.Butkevich, L.G.Dedenko, S.Kh.Karaevsky,
A.A.Mironovich, A.L.Provorov, I.M.Zheleznykh*

Institute for Nuclear Research of Russian Academy of Sciences, Moscow

| | |
|--|-----|
| INTRODUCTION | 660 |
| NEUTRINO-NUCLEON CROSS SECTION | |
| AT ENERGIES OF 10^2 — 10^{12} GeV | 662 |
| Neutrino-Nucleon Cross Section in the Standard Model | 662 |
| Parton Distribution in Nucleon at $x > 10^{-5}$ and the Neutrino-Nucleon Cross Section | 662 |
| Possible Parametrizations of the PDF in the Small- x Region and the νN Cross Section at Ultrahigh Energy | 664 |
| THE ACOUSTIC PULSE CAUSED BY THE CASCADE WITH THE ENERGY OF 10 PeV | 665 |
| ESTIMATIONS OF SADCO EFFECTIVE VOLUME | 666 |
| RESULTS OF THE RAMAND THRESHOLD ANALYSIS | 667 |
| RAMAND DETECTION OF AGN NEUTRINOS | 672 |
| CONCLUSIONS | 672 |
| REFERENCES | 674 |
| M.A.MARKOV AND HIGH-ENERGY NEUTRINO ASTRONOMY | 675 |
| REFERENCES | 676 |

PROSPECTS FOR RADIOWAVE AND ACOUSTIC DETECTION OF ULTRA- AND SUPERHIGH ENERGY COSMIC NEUTRINOS (CROSS SECTIONS, SIGNALS, THRESHOLDS)

*A.V.Butkevich, L.G.Dedenko, S.Kh.Karaevsky,
A.A.Mironovich, A.L.Provorov, I.M.Zheleznykh*

Institute for Nuclear Research of Russian Academy of Sciences, Moscow

In the framework of the Standard Model the neutrino-nucleon cross section is calculated for the energy range 10^2 — 10^{12} GeV. At neutrino energy of 10^6 GeV the new result is 50 % above the previous results. The amplitude of acoustic signal caused by the electron-hadron cascade induced by neutrino interacting with electrons and nucleons in water was recalculated in terms of the quark-gluon string model at energies of 10^6 — 10^8 GeV. This amplitude is about twice as much as the foregoing estimates. It is shown that a 1 km^2 radiowave neutrino detector (RAMAND) set up in Central Antarctica (at the South Pole or Vostok Station) should be sensitive to the predicted diffuse fluxes of AGN neutrinos at energies above a hundred TeV. Another planning cubic kilometer-scale (KM3) neutrino telescope — the deep underwater neutrino detector SADCO in the Mediterranean Sea — could search for cosmic neutrinos of energies higher than 10^7 — 10^8 GeV.

В рамках стандартной модели рассчитано поперечное сечение взаимодействия нейтрино с нуклонами в области энергий 10^2 — 10^{12} ГэВ. Для энергии нейтрино 10^6 ГэВ новый результат на 50 % выше результатов предыдущих расчетов. Рассчитана амплитуда акустического сигнала от электрон-адронного каскада с энергией 10^6 — 10^8 ГэВ, производимого в воде нейтрино, которые взаимодействуют с электронами и нуклонами, и описываемого моделью кварк-глюонных струн. Эта амплитуда в два раза выше результата более ранних оценок. Показано, что радиоволновой нейтринный детектор РАМАНД площадью 1 км^2 , установленный в центральной Антарктиде (на Южном полюсе или станции «Восток») может быть чувствителен к предсказанным диффузным потокам нейтрино с энергиями выше 100 ТэВ из ядер активных галактик. Акустический нейтринный телескоп САДКО в Средиземном море с объемом детектирования более 1 км^3 может быть предназначен для поиска космических нейтрино с энергией выше 10^7 — 10^8 ГэВ.

1. INTRODUCTION

The search for neutrino fluxes from the cosmic space and their detection in the wide energy interval $10\text{--}10^{11}$ GeV can be carried out if to construct large-scale neutrino telescopes — detectors with effective registration volumes of $10^7\text{--}10^{10}$ m³. Deep underwater optical neutrino telescopes, BAIKAL, NESTOR (Mediterranean), and Antarctic ice detector AMANDA (South Pole) are under construction now. However the neutrino induced electron-photon and hadron cascades could be registered not only by optical but the acoustic emission in water and the radiowave emission in cold ice.

Energy thresholds for the radiowave and acoustic detection are a few orders of value higher than $E_{\text{thr}} \sim 10\text{--}50$ GeV for the optical underwater detection. But due to weak absorption of acoustic (radiowave) signals in water (Antarctic ice) effective volumes of acoustic (radiowave) neutrino targets could be of an order of the cubic kilometer and larger (KM3-detectors) that is very important for goals of the superhigh energy neutrino astrophysics.

The study of the νN -interaction cross section at high and ultrahigh energies is important from a theoretical as well as experimental point of view. In order to solve an interesting problem, namely — what is the maximal energy of cosmic ray neutrinos — one has to know these cross sections for neutrino energies greater than 10^{11} GeV, because there exist some arguments that the upper bound of the neutrino energy spectrum can reach 10^{19} GeV [1]. Knowledge of these cross sections is also necessary for the interpretation of underground, future underwater and Antarctic ice neutrino experiments. In the present work neutrino-nucleon cross sections for neutrino energy $E_\nu \leq 10^{12}$ GeV are considered. The comparison of the νN cross section and the cross section of the reaction $\nu_e + e^- \rightarrow W^- \rightarrow X$ near resonant energy $6 \cdot 10^6$ GeV is made.

The acoustic detection of elementary particles was suggested by G.A.Askaryan in the 50's [2]. A possibility of deployment of the deep ocean acoustic detector to search for ultrahigh-energy (UHE) neutrinos (with energies above 10 PeV) had been discussed almost 20 years ago by G.A.Askaryan and B.A.Dolgoshein [3], T.Bowen [4] and J.G.Learned [5]. The prediction of considerable UHE neutrino fluxes from the active galactic nuclei (AGN) by Stecker et al. [6] supported much the idea of deployment of the large-scale cosmic neutrino detectors and in particular, the acoustic neutrino telescope [7]. The deep underwater acoustic neutrino telescope SADCO (Sea Acoustic Detector of Cosmic Objects) with the threshold energy above 5 PeV was recently suggested to be deployed at the depth of 3.5—4 km in the Ionian Sea near Pylos (Greece)

just at the site of the optical neutrino telescope NESTOR [8—10]. The search for UHE neutrinos via a detection of an acoustic bipolar pulse caused by water heating due to energy deposits in the electron-hadron cascades initiated by interactions of these neutrinos of all flavors with nucleons in matter and particularly by the resonance interactions of electron-antineutrino with electrons is the main goal of the SADCO project. The sensitive volume of the SADCO neutrino telescope should be not less than 10^8 m^3 if dozens of events per year caused by neutrinos with the resonance energy are expected. Thus new estimates of an acoustic signal are of importance. The sound pressure level and the duration of the acoustic bipolar pulse produced by the electron-hadron cascades are of great interest. The results of calculations of characteristics of acoustic pulse produced by the electron-hadron cascade with the energy of 10 PeV in sea water are presented in this paper. Estimations of effective detection volumes of SADCO for cascade energies of 10^7 — 10^8 GeV as functions of acoustic signal and hydrophone numbers are also given.

About 30 years ago Askaryan proposed a new method for detection of high-energy particles by means of the Cherenkov coherent radiowave emission from the negative charge excess of electromagnetic showers generated in air or dense media [11]. The charge imbalance of a shower is created by the Compton scattering of shower photons on atomic electrons, the annihilation of shower positrons in flight and the knock-on process. The percentage of negative charge excess amounts to ~20% at the shower maximum. The resulting Cherenkov emission by excess electrons is coherent at wavelengths larger than the shower lateral dimension, i.e., in the radiowave region. In spite of the very low frequencies compared with visible light, this emission should be observable for sufficiently high primary energy because the radiated power scales with the square of the shower size.

After a while, interest in the idea of Askaryan was renewed by the suggestion to detect high-energy (HE) neutrinos in cold Antarctic ice, which has very low radiowave absorption at temperatures below $-50 \text{ }^\circ\text{C}$ [12]. It was argued that a radioantenna array placed on the glacier surface in Central Antarctica could provide an effective target volume of the order of 10^9 — 10^{10} m^3 for cosmic neutrinos with energies above $\sim 100 \text{ TeV}$ [12—14].

In this paper we present the results of a detailed threshold analysis for such a detector, taking account of radiowave absorption in ice, the results of calculations of an expected neutrino event rate in a radiowave detector for different anticipated HE neutrino fluxes.

2. NEUTRINO-NUCLEON CROSS SECTION AT ENERGIES OF 10^2 — 10^{12} GeV

2.1. Neutrino-Nucleon Cross Section in the Standard Model. The cross section for deep inelastic charged current neutrino-nucleon process in the standard model of electroweak interaction is given by

$$\frac{d\sigma^{\nu, \bar{\nu}}}{dx dy} = \frac{G^2}{2\pi} \frac{s}{(s_\omega xy + 1)^2} \left[\frac{y^2}{2} 2xy F_1(x, Q^2) + (1-y) F_2(x, Q^2) \right. \\ \left. \pm y \left(1 - \frac{y}{2} \right) xF_3(x, Q^2) \right], \quad (1)$$

where $s = (p_\nu + p_N)^2$, $s_\omega = s/3m_\omega^2$ (m_ω is the W -boson mass), x is the fraction of the nucleon momentum carried by the quark which interacts with neutrino, y is the fraction of the neutrino energy which is transferred to the quark, $Q^2 = -t$ is the transferred four-momentum squared. The nucleon structure functions (SF) $F_2(x, Q^2)$, $2xF_1(x, Q^2)$, and $xF_3(x, Q^2)$ can be expressed in terms of the parton distribution functions (PDF) in the nucleon. The main contribution to the total cross section at $s \geq m_\omega^2$ comes from the region $s_\omega xy < 1$, i.e., $Q^2 \leq m_\omega^2$ and hence $x \leq m_\omega^2/s$ due to the presence in (1) of the W -boson propagator. Because of the very weak dependence of $F_i(x, Q^2)$ on Q^2 for estimation one can make the substitutions $F_2(x, Q^2) \approx F_2(x, m_\omega^2)$, $2xF_1(x, Q^2) \approx 2xF_1(x, m_\omega^2)$, and $xF_3(x, Q^2) \approx xF_3(x, m_\omega^2)$. For $x \rightarrow 0$, $xF_3(x, m_\omega^2) \rightarrow 0$ and if $F_2(x, m_\omega^2) \rightarrow \text{const}$ at $x \rightarrow 0$, then in LO approximation the asymptotic behaviour of total cross section will be $\sim F_2(0, m_\omega^2) \ln(s_\omega)$. So, at $s_\omega \gg 1$ the neutrino and antineutrino cross sections for scattering on an isoscalar target become equal and are determined by the value of $F_2(x, Q^2)$ at $x \rightarrow 0$.

2.2. Parton Distribution in Nucleon at $x > 10^{-5}$ and the Neutrino-Nucleon Cross Section. The fixed target lepton-nucleon scattering experiments and the H1 and ZEUS [15—16] detectors of HERA have measured the proton SF $F_2(x, Q^2)$ covering the very large kinematic range of $0.3 \leq Q^2 \leq 10^4$ GeV and $2 \cdot 10^{-4} < x < 1$. The steep rise (as $\sim x^{-\lambda}$ with $\lambda \sim 0.3$ – 0.4) of the SF F_2 with x decreasing is observed at x value below 10^{-1} and up to Q^2 values of about

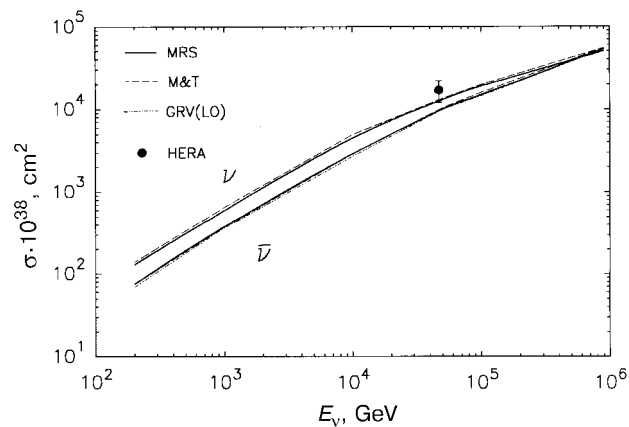


Fig.1. Using the PDF of GRV [17], MT [18] and MRS(A) [19] the νN - and $\bar{\nu}N$ -interaction cross sections for energies up to 10^6 GeV have been calculated. The results of these calculations are given in the figure

10^3 GeV². These results have generated considerable theoretical interest in small- x physics. Several sets of the PDF [13—15] were obtained from a global analysis of these data. These sets are based on NLO QCD calculations and are valid for $x > 10^{-5}$ and $4-5 \leq Q^2 \leq 10^6-10^8$ GeV². Using the PDF of GRV [17], MT [18] and MRS(A) [19] we have calculated the νN - and $\bar{\nu}N$ -interaction cross sections for energies up to 10^6 GeV. The results of these calculations are given in Fig.1.

At low energies ($E_\nu < 10^3$ GeV) these results accord well with experimental data. At energies $E_\nu = 10^6$ GeV the discrepancy between cross sections calculated for different sets is not more than of 12%. The $\sigma_{\nu N}$ (MRS) calculated with the MRS(A) PDF are shown in Fig.2; νN cross sections which have been obtained in [20] are given in the same figure for comparison. The results of the previous works [21—23] that have been obtained using the EHLQ PDF[24] are shown in this figure, too. At energy $E_\nu = 10^6$ GeV the σ_ν (MRS) is 45% above the old results [21—24] and less than the cross section of [20] by a factor of 1.60. So, the appreciable increase of the νN cross sections in the range $E_\nu = 10^5-10^6$ GeV is due to the steeper rise of the MRS(A) PDF respect to the EHLQ PDF with decreasing x .

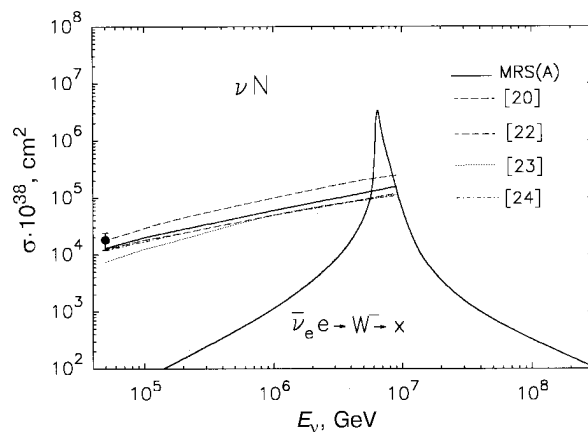


Fig.2. Comparison of the present neutrino-nucleon cross sections with previous results and resonant cross section

2.3. Possible Parametrizations of the PDF in the Small- x Region and the νN Cross Section at Ultrahigh Energy.

The ultrahigh energy ($E_\nu > 10^6$ GeV) neutrino-nucleon cross section depends on the behaviour of the SF in the small- x region. In the present work we have used two approaches to estimate the SF at $x \rightarrow 0$. In the first approach (case A) the MRS(A) PDF were extrapolated from the region $x > 10^{-5}$ and $Q^2 \leq 10^6$ GeV² into the region of smaller x 's and greater Q^2 's. The $\sigma_{\nu N}$ (A) obtained with these PDF are listed in Table 1. In the second approach (case B) we used the solutions of the Altarelli-Parisi equations for moments of the singlet and nonsinglet SF and for the gluon distribution in LO approximation [25] with input distributions $g(x, Q_0^2)$, $q_s(x, Q_0^2) \sim x^{-0.3}$ (as in the case of the MRS(A) PDF). The leading singularity of input moments, corresponding to a simple pole at $n=1.3$, controls the behaviour of the

Table 1. The ultrahigh energy neutrino-nucleon cross section $\sigma_{\nu N} \cdot 10^{38}$ cm²

| E (GeV) | 10^7 | 10^8 | 10^9 | 10^{10} | 10^{11} | 10^{12} |
|-----------|-------------------|-------------------|-------------------|-------------------|-------------------|-------------------|
| Case (A) | $1.77 \cdot 10^5$ | $4.73 \cdot 10^5$ | $1.19 \cdot 10^6$ | $2.83 \cdot 10^6$ | $6.41 \cdot 10^6$ | $1.40 \cdot 10^7$ |
| Case (B) | $1.77 \cdot 10^5$ | $4.75 \cdot 10^5$ | $1.21 \cdot 10^6$ | $2.99 \cdot 10^6$ | $7.15 \cdot 10^6$ | $1.67 \cdot 10^7$ |

$F_i^{as}(x, Q^2)$ at small x . Besides we took into account the standard QCD singularity at $n=1$. The cross sections σ_{vN} (B) obtained by using the SF F_i (MRS) at $x > 10^{-5}$ and the SF F_i^{as} at $x < 10^{-5}$ (they have been smoothly 'sewn' at $x = 10^{-5}$) are listed in Table 1. σ_{vN} (A) is $\sim 20\%$ above the σ_{vN} (B) at energy $E = 10^{12}$ GeV.

3. THE ACOUSTIC PULSE CAUSED BY THE CASCADE WITH THE ENERGY OF 10 PeV

The bipolar acoustic signal was calculated taking into account the energy deposits by the electron-hadron cascade estimated in terms of the quark-gluon string model [10]. Figure 3 shows the bipolar acoustic pulses caused by the cascade with the energy of 10 PeV at a distance of 400 m from the cascade core allowing for the sound absorption in the sea water.

Curve 1 was taken from [5], curve 2 — from [26] and curve 3 displays our calculations [27]. All signals were recalculated to the parameters of the NESTOR polygon (4 km depth and 14 °C temperature of water). It should be noted that in paper [28] the new estimate of the acoustic pressure of 250 μPa

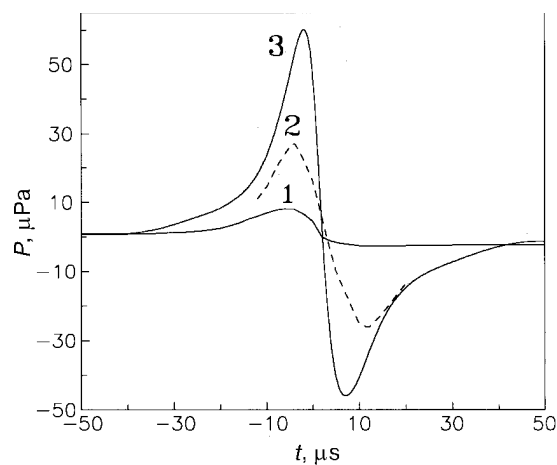


Fig.3. The acoustic pulse in sea water at a distance of 400 m from a cascade with the energy of 10 PeV. 1 — Learned J. [5]; 2 — Askaryan G. et al. [26]; 3 — Denenko L. et al. [27]

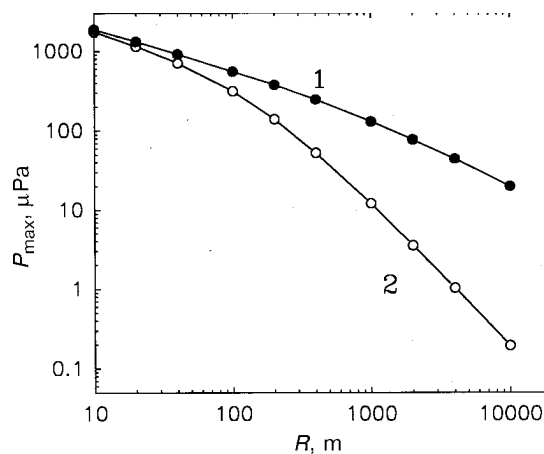


Fig.4. The dependence of an acoustic signal maximal amplitude on a distance from the cascade shower without absorption (1) and with absorption taken into account (2)

at a distance of 40 m from the cascade core was given. This value corresponds to the pressure of 80 μPa at a distance of 400 m but not allowing for the absorption of the sound. Figure 3 displays that the amplitude of our signal (3) is approximately twice as much as the pulse (2) [26]. This can be accounted for the more narrow radial distribution of electrons in the cascade [10] in comparison with an approximation used in [26].

Thus according to different estimates the amplitude of acoustic pulse caused by the electron-hadron cascade with the energy of 10 PeV in sea water can vary from 25 up to 60 μPa at a distance of 400 m from the cascade core allowing for the sound absorption. The main fraction of the acoustic signal energy is distributed inside the frequency band of 2-30 kHz in [26] and inside the band of 4-50 kHz in case of our pulse (3) [27]. Figure 4 illustrates the dependence of the maximal acoustic pressure P_{\max} on the distance from the cascade with the energy of 10 PeV. Curve 1 is calculated disregarding absorption of sound in water and curve 2 takes into account this absorption. Figure 5 shows the dependence of acoustic pulse on displacement of hydrophone along cascade axis for perpendicular distances of 100 m (1), 400 m (2), 1,000 m (3), 2,000 m (4), and 3,000 m (5) from the cascade axis.

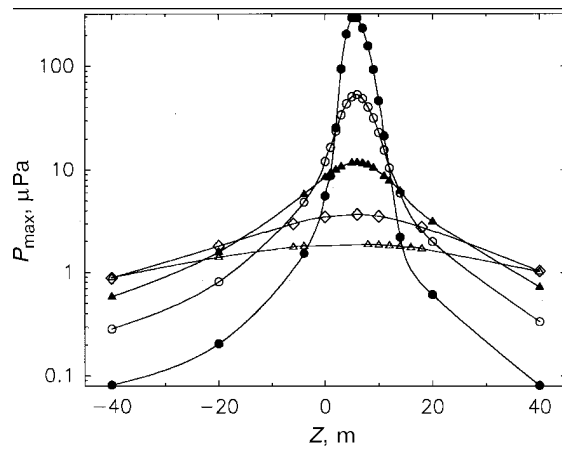


Fig.5. The dependence of an acoustic signal amplitude on a displacement Z along the cascade axis. Symbols \bullet : $R = 100$ m; \circ : $R = 400$ m; \blacktriangle : $R = 1000$ m; \diamond : $R = 2000$ m; \triangle : $R = 3000$ m. $E_0 = 10$ PeV

4. ESTIMATIONS OF SADCO EFFECTIVE VOLUME

A cascade produces an acoustic signal localized in a thin divergent disk which is perpendicular to cascade axis (e.g., see Fig.6). Acoustic detection effective volume V_{eff} may be evaluated as the volume of region where the acoustic signal from cascade is higher than the chosen threshold (see Fig.7). The ratio of this effective volume to the geometrical one (which is $\sim R^3$) is rather small (e.g., 0.6—1 %, see Table 2).

Table 2 shows this effective volume as a function of maximal distance of detection R_{max} , acoustic signal level P and number of hydrophones n for signal-to-noise ratio $S/N = 1$ and noise level of $400 \mu\text{Pa}$.

It can be seen from this table that the effective volume $V_{\text{eff}} \sim 5 \cdot 10^7 \text{ m}^3$ may be got for cascade energy of 10^{16} eV if hydrophones number in compact array would be not less than 2,000 (for $S/N = 1$). In case of cascade energy above 10^{17} eV hydrophones number would be considerably less (~ 400) and an effective volume will increase up to 10^9 m^3 .

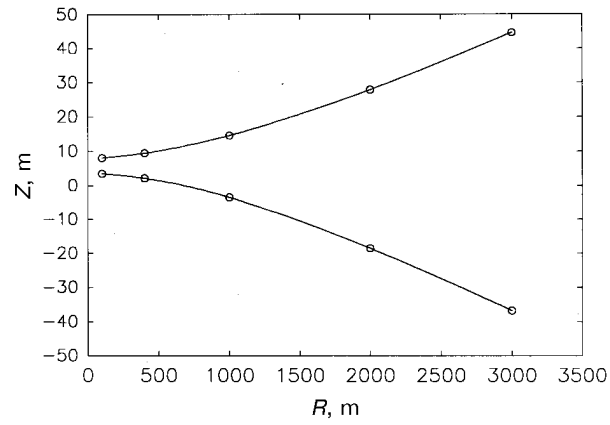


Fig.6. Cross section of divergent disk of acoustic radiation at -6 dB level for 10 PeV cascade. R is the distance from cascade axis in perpendicular direction

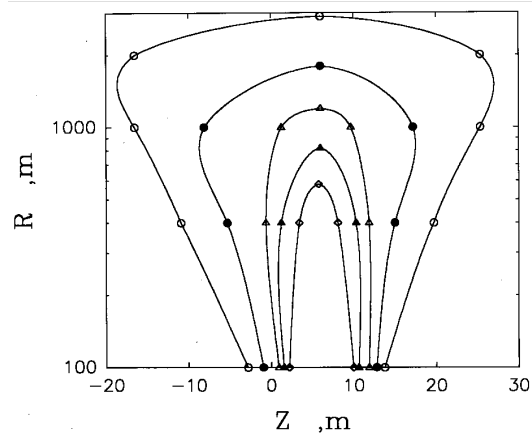


Fig.7. Contours of constant level of acoustic signal for 10 PeV cascade. Symbols \circ : 2 μPa , \bullet : 20 μPa , \triangle : 10 μPa , \blacktriangle : 20 μPa , \diamond : 40 μPa

Table 2. Dependence of acoustic detection effective volumes upon distance, min level of signal, number of hydrophones and ratio of effective volume to geometrical one

| | | | | | |
|---|------|------|------|-------|-------|
| Effective volumes, $V_{\text{eff}} \cdot 10^{-7}, \text{m}^3$ | 0.53 | 1.6 | 4.3 | 21 | 95 |
| Max, distance, R, m | 600 | 800 | 1200 | 1800 | 2900 |
| Min level of signal, P, μPa | 40 | 20 | 10 | 4 | 2 |
| Number of hydrophones, n | 100 | 400 | 1600 | 10000 | 40000 |
| Ratio, $V_{\text{eff}}/V_g, \%$ | 0.59 | 0.75 | 0.59 | 0.86 | 0.93 |

5. RESULTS OF THE RAMAND THRESHOLD ANALYSIS

We consider a radiowave antarctic neutrino detector RAMAND as a number of downward-looking antennae disposed on several dozen meters triangular grid enclosing a glacier area of the order of 1 km^2 . The antennae sample Cherenkov radio pulses from ice, which would provide well-defined conic-type images on the grid (the Cherenkov angle is equal to 56° in ice) [12—14].

A numerical real time computation of the radiowave emission from electromagnetic showers developed in the totally transparent ice [29] gives the following parametrization of the electric field spectrum at the Cherenkov angle:

$$R |\mathbf{E}(\omega, R, \theta_c)| = \frac{0.55 \cdot 10^{-7} (\nu/\nu_0)}{1 + 0.4(\nu/\nu_0)^2} \frac{E_0}{1 \text{ TeV}} (\text{V/MHz}). \quad (2)$$

Here ν is the frequency, R is the distance from the shower, E_0 is the incident electron (photon) energy, $\nu_0 = 500 \text{ MHz}$ (the result of [29] was divided by 2 to define the Fourier transform as $\mathbf{E}(\omega) = \int dt \mathbf{E}(t) \exp(i\omega t)$).

Radiowave attenuation in the real ice strongly depends on the wavelength, as well as on the ice temperature. Therefore, we have used the original data on radiowave absorption in ice [30] together with the results of temperature profile measurements in a superdeep bore hole at the Vostok Antarctic Station [31] to calculate the total attenuation of a shower radio pulse after vertical propagation from a given depth to the ice surface (Fig.8).

To obtain the threshold energy for the one-channel radiowave detection of electromagnetic showers we need to consider in some detail a process of radio-

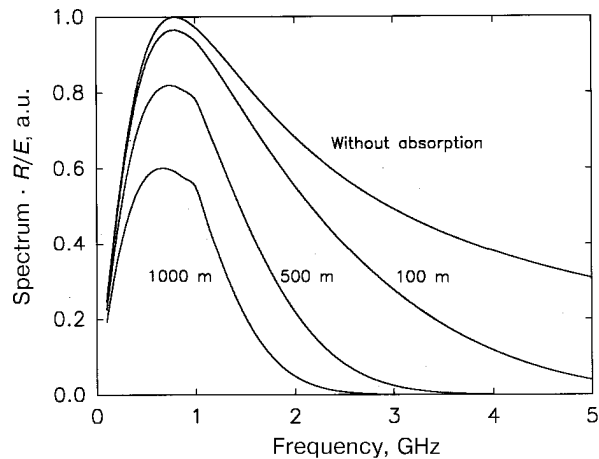


Fig.8. Radio pulse spectrum after vertical propagation from a given depth (the maximum value is equal to $43.5 \text{ nV}/(\text{MHz} \cdot \text{TeV})$)

pulse transformations by a receiving antenna and its preamplifier (active filter). The relation between output antenna voltage $V(\omega)$ and incident electric field $\mathbf{E}(\omega)$ is given by

$$V(\omega) = \mathbf{R}_A(\omega) \mathbf{E}(\omega), \quad (3)$$

where $\mathbf{R}_A(\omega)$ is the reception transfer function of antenna. As is recognized, the so-called TEM horn is the most promising broad-band antenna for impulsive field measurements (for instance, see Ref.32). Its reception transfer function has approximately constant magnitude and linear phase dependence over the frequency range from a hundred MHz to several GHz. As one can see (Fig. 8), the shower radio pulse spectrum has the same band of wavelengths. Therefore, the TEM horn will produce an output voltage that is a high fidelity replica of the shower electric field in the time domain. For example, the $1 \times 1 \text{ m}^2$ arcsine TEM horn specially designed for the neutrino radiowave experiments has $R_A \approx 0.14 \text{ V}/(\text{V}/\text{m})$ for a normal incident field in air. The reception pattern of this antenna is rather broad with the half-amplitude beamwidths of about 90° in both E and H planes for an incident electromagnetic pulse of 1 ns duration [14].

The conventional definition of a signal-to-noise ratio at the filter output is [33]

$$\frac{S}{N} = \frac{\text{peak instantaneous output signal power}}{\text{output noise power}}. \quad (4)$$

The maximum of (4) occurs when the filter transfer function is proportional to the complex conjugation of the input filter voltage $V^*(\omega)$ («matched filter»). The maximum value is

$$[S/N]_{\max} = \frac{2}{N_0} \int_{-\infty}^{+\infty} \frac{d\omega}{2\pi} |V(\omega)|^2, \quad (5)$$

where N_0 is the one-sided white noise power density at the filter input. From (3) and (5) we obtain for the normal incident shower radio pulse received by a TEM horn in ice:

$$[S/N]_{\max} = \frac{2}{N_0} \varepsilon R_A^2 \int_{-\infty}^{+\infty} \frac{d\omega}{2\pi} |\mathbf{E}(\omega, R, \theta_c)|^2, \quad (6)$$

where ε is the relative permeability of ice (R_A rises by a factor of $\sqrt{\varepsilon}$ in medium). If the antenna impedance is equal to the load (filter) one,

$$N_0 = kT_N Z_L. \quad (7)$$

Here $k = 1.381023$ J/K is the Boltzmann constant, T_N is the noise temperature and Z_L is the load impedance. Using the parametrization (2) and taking into account the radiowave absorption in ice for vertical pulse propagation from 100 m depth, we find for $Z_L = 50$ Ohm and $\sqrt{\varepsilon} = 1.8$ (ice refraction coefficient):

$$[S/N]_{\max} \cong 0.1 \frac{E_0^2(\text{TeV})}{T_N(\text{K})} \left(\frac{R_A}{0.14\text{m}} \right)^2. \quad (8)$$

For the signal-to-noise ratio of unity, $T_N = 300$ K (according to the antarctic noise measurements [34]) and $R_A = 0.14$ V/(V/m) the shower threshold energy E_{th} is approximately equal to 55 TeV. This is a factor of 7 lower than the result obtained by Zas, Halzen, and Stanev [29]. They performed the threshold estimation for a half-wave dipole antenna adapted for the narrow-band receiving technique of EAS radio detection experiments. Hence, the use

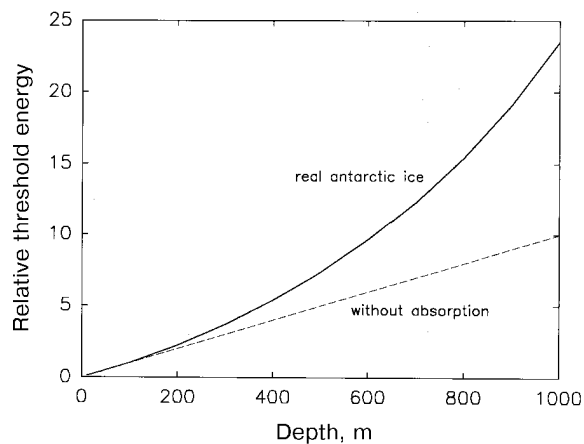


Fig.9. Relative threshold dependence on depth (E_{100} is taken to be unity)

of a broad-band TEM horn together with a matched filter results in the significant decrease of the threshold energy.

Figure 9 shows the calculated dependence of the relative threshold energy on the shower production depth.

6. RAMAND DETECTION OF AGN NEUTRINOS

We calculated the expected event rate in a 1 km^2 radiowave detector for the different existing models of AGN neutrino production, assuming $E_{100} = 55 \text{ TeV}$ and $R_{\min} = 100 \text{ m}$ (for comparative discussion of the models see Refs. 35,36). The results are given in Table 3. The expected background from atmospheric neutrinos [37] will be ~ 20 events per year.

These figures can be compared with the predicted muon event rate in a 10^4 m^2 optical underwater neutrino telescope, such as DUMAND II, NESTOR or NT-200, which are under construction now. According to [36] at muon energies above 1 TeV the rate will be for Ref.38 ~ 30 per year and for Ref.39 from 160 to 800, decreasing by several times at 10 TeV. Ultrahigh energy neutrinos from AGN can be detected by DUMAND II due to the Glashow resonance reaction with the rate for Ref.38 about several dozen events per year [40].

Table 3. Expected event rate for the different models of AGN neutrino production

| Diffuse neutrino fluxes from AGN by | Expected event rates ($S/N = 1$), year ⁻¹ km ⁻² |
|-------------------------------------|---|
| Stecker et al., 1992 | 110 |
| Szabo and Protheroe, 1992 (max) | 2800 |
| Szabo and Protheroe, 1992 (min) | 730 |
| Biermann, 1992 | 110 |
| Siroka and Begelman, 1992 | 100 |

7. CONCLUSIONS

The charged current neutrino-nucleon cross sections have been calculated for incoming neutrino energies in the range of 10^2 – 10^{12} GeV. At $s_\omega \gg 1$ the $\sigma_N^{\nu}(E) = \sigma_N^{\bar{\nu}}(E)$. Their behavior is determined by the behavior of SF $F_2(x, Q^2)$ for $x \rightarrow 0$. Using the PFD of the GRV, MT and MRS we have calculated $\sigma^{\nu, \bar{\nu}}$ up to $E_\nu = 10^6$ GeV. The appreciable νN cross section increase (compared with previous results) at energies $E_\nu = 10^5$ – 10^6 GeV is due to the steeper rise of these PDF for $x \rightarrow 0$. The ultrahigh energy neutrino-nucleon cross sections have been calculated for two cases of the behaviour of the SF at $x \rightarrow 0$. The results are different not more than by 20 % at $E_\nu = 10^{12}$ GeV.

The results of the measurements [8,9,10] carried out in the Ionian Sea near Pylos (Greece) in 1991 and 1992 displayed the relatively low level of acoustic noises of $12 \mu\text{Pa}/\text{Hz}^{0.5}$ at the frequency band of 15–30 kHz and rather high temperature of water of about 14°C at depths of 0.2–4 km, that makes this polygon near Pylos very attractive for deployment of the acoustic neutrino telescope SADCO.

Our calculations of the acoustic signal yield the amplitude of pulse of $60 \mu\text{Pa}$ for the electron-hadron cascade with the energy of 10 PeV at the distance of 400 m from the cascade core allowing for the sound absorption in the sea water. This amplitude is a few times as much as the foregoing estimates [5,26]. The calculated frequency spectrum of the acoustic pulse is localized inside the range of 4–50 kHz which is rather attractive from the point of view both of a detection and the minimal noise level in the sea.

In our calculations of acoustic signal we have not taken into account the LPM effect which is small at energies below 10^{16} eV. But at higher energies the

LPM effect becomes significant in case of electron-photon cascades in water. This is particularly important for the neutrino reactions with electron (positron) production. Our calculations show that the cascade length in water increases proportionally to $(E/10^{16} \text{ eV})^{0.5}$ due to the LPM effect and density of energy deposits also grows with the same factor. Especially it should be stressed that the sensitive volume in the near field also grows with the same factor — $(E/10^{16} \text{ eV})^{0.5}$. Thus both the results of measurements [8,9,10] and of calculations of the acoustic signal are of interest for investigations of UHE neutrino fluxes from the active galactic nuclei by the acoustic method. In particular the search for resonant interactions of cosmic electron-antineutrino with electrons in water at the energy of 6.4 PeV is of importance.

In this paper we have shown that a 1 km^3 radiowave neutrino detector established in Central Antarctica (at the South Pole or Vostok Station) should be sensitive to the predicted diffuse fluxes of AGN neutrinos at energies above a hundred TeV. For some production models AGN neutrinos would be effectively detected in the broad energy region up to 1 PeV, that gives, in principle, a possibility of determining the spectrum shape.

The Russian Foundation for Basic Research is thanked for a support (Grant No.96-02-18594).

REFERENCES

1. **Markov M.A., Zheleznykh I.M.** — Proc. 1979 Dumand Summer Workshop at Khabarovsk and Lake Baikal, Ed. J.Learned, 1980, p.177.
2. **Askaryan G.A.** — Atomnaya energiya (in Russian), 1957, v.3, p.152.
3. **Askaryan G.A., Dolgoshein B.A.** — Report on the 1976 DUMAND Summer Workshop, Hawaii, September, 1976; Preprint P.N.Lebedev Physical Institute (in Russian) No.160; ZhETF Pis. Red., 1977, v.25, p.232.
4. **Bowen T.** — Conference Papers, 15th Intern. Cosmic Ray Conf., Plovdiv, 1977, v.6, p.277.
5. **Learned J.** — Phys. Rev., 1979, v.D19, p.3293.
6. **Stecker F.W. et al.** — Proc. 3d Int. Workshop on Neutrino Telescopes, Venezia, 1991, p.487.
7. **Learned J., Stanev T.** — Proc. 3d Int. Workshop on Neutrino Telescopes, Venezia, 1991, p.473.
8. **Butkevich A. et al.** — Proc. 2nd Int. Conf. on Trends in Astroparticle Physics, 1991, Aachen, Germany, Tubner-Texte für Physik, 1994, v.B28, p.128.
9. **Butkevich A. et al** — Proc. 2nd NESTOR Int. Workshop, Pylos, Greece, 1992, p.345; **Trenikhin A.**, ibidem, 1992, p.354.
10. **Karaevsky S. et al.** — XXIII Int. Cosmic Ray Conf., Calgary, 1993, v.4, p.550.
11. **Askaryan G.A.** — Zh. Exp. Teor. Fiz., 1961, v.41, p.16; ibid, 1965, v.48, p.988.
12. **Gusev G.A., Zheleznykh I.M.** — ZhETF Pis. Red., 1983, v.38, p.505; **Markov M.A., Zheleznykh I.M.** — Nucl. Inst. Methods, 1986, v.A248, p.242.

13. **Ralston J.P., McKay D.W.** — Nucl. Phys. B (Proc. Suppl.), 1990, v.14A, p.356.
14. **Boldyrev I.N. et al.** — In: Proc. 3rd Int. Workshop on Neutrino Telescopes, Ed. Milla Baldo Ceolin, Venezia, 1991, p.337.
15. **Abt I. et al.** — Nucl.Phys., 1993, v.B407, p.515 [11].
16. **Derrick M. et al.** — Phys.Lett., 1993, v.B136, p.412
17. **Gluck M. et al.** — Preprint DO-TH 90/07, 1990.
18. **Morfin J.G. et al.** — Z.Phys.C, 1991, v.52, p.13
19. **Martin A.M. et al.** — Preprint RAL-94-055, 1994.
20. **Ralston J.P. et al.** — Phys. Rev. Lett., 1994, v.12, p.21.
21. **Eichten E. et al.** — Rev.of Mod. Phys., 1984, v.56, p.579.
22. **Reno M.N. et al.** — Phys.Rev., 1988, v.D37, p.657.
23. **McKay W. et al.** — Phys.Lett., 1986, v.B167, p.103.
24. **Butkevich A.V. et al.** — Z.Phys., 1988, v.C39, p.241.
25. **Altarelli G.** — Phys. Reports, 1982, v.C81, p.1.
26. **Askaryan G.A., Dolgoshein B.A., Kalinovsky A.N., Mokhov N.V.** — Nucl. Inst. Meth., 1979, v.164, p.267.
27. **Dedenko L.G. et al.** — Izv. RAN (ser. fiz.), 1994, v.58, p.146.
28. **Learned J., Wilkes R.J.** — XXIII Int. Cosmic Ray Conf., Calgary, 1993, v.4, p.538.
29. **Zas E., Halzen F., Stanev T.** — Phys. Lett., 1991, v.B257, p.432; Phys. Rev., 1992, v.D45, p.362.
30. **Bogorodsky V.V., Gavrilov V.P.** — Ice: Physical Properties. Modern Methods of Glaciology, Leningrad, 1980.
31. **Vostretsov R.N. et al.** — In: Data of Glaciological Studies, Moscow, 1984, v.51, p.172.
32. **Lawton R.A., Ondrejka A.R.** — NBS Technical note 1008, U.S. Department of Commerce, 1978.
33. **Cook C.E., Bernfeld M.** — Radars Signals. An Introduction to Theory and Application, New York — London, 1967.
34. **Bogomolov A.F. et al.** — In: Proc. 20th Int. Cosmic Ray Conf., Moscow, 1987, v.6, p.472.
35. **Berezinsky V.** — Phil. Trans. R. Soc. Lond., 1994, v.A346, p.93.
36. **Stanev T.** — In: Proc. 23rd Int. Cosmic Ray Conf., Calgary, 1993, Invited, rapporteur and highlight papers, p.503.
37. **Volkova L.V., Zatsepin G.T.** — Yad. Fiz., 1983, v.37, p.353; Izv. Acad. Nauk SSSR (Fiz. Ser.), 1985, v.49, p.1386; **Volkova L.V.**, 1994, private communication.
38. **Stecker F.W., Done C., Salamon M.H., Sommers P.** — In: Proc. Workshop High Energy Neutrino Astronomy, Eds. Stenger V.J., Learned J.G., Pakvasa S., Tata X., Singapore, 1992, p.1.
39. **Szabo A.P., Protheroe R.J.**, *ibid.* p.24.
40. **Learned J.G., Stanev T.** — In: Proc. 3rd Int. Workshop on Neutrino Telescopes, Ed. Milla Baldo Ceolin, Venezia, 1991, p.473.

M.A.MARKOV AND HIGH-ENERGY NEUTRINO ASTRONOMY

In 1960 at the 10th Rochester Conference Moisey Alexandrovich Markov had suggested an idea of the underground experiments for the detection of the high energy atmospheric and extraterrestrial neutrinos to study a number of the

fundamental problems of particle physics and astrophysics. The possibility of the neutrino detection using Cherenkov light radiation from the muons and cascades produced in neutrino reactions «in an underground lake or deep in an ocean» was also pointed out [1].

During the last several decades a new branch of physics and astrophysics — neutrino astronomy — initiated by Markov has been developed. Since the first detection of the atmospheric neutrinos with energies 1—100 GeV in underground neutrino experiments in gold mines of the South Africa and India, the target mass scale of the instruments — underground neutrino telescopes — has grown to 5×10^4 tons (Super-Kamiokande). An artificial water target was used for SuperK instead of the «underground lake». In fact neutrino telescopes have become universal instruments for the investigation of the microworld (e.g., in the search for the proton decay), as well as searching for cosmic objects (e.g., solar neutrinos, supernova neutrinos, WIMPS, monopoles, etc.). The Baksan neutrino telescope with 300 tons of scintillator is one of such instruments.

However to search for the ultrahigh energy (greater than 10^6 GeV) astrophysical neutrino sources, i.e., sites of the activity of the specific cosmic accelerators in the Universe, neutrino telescopes of the effective detection volume of a cubic kilometer or more are necessary [2]. In the Soviet Union (Russia) the R&D program for the large-scale neutrino telescopes in the Ocean and in Antarctica was developed under the leadership of M.A.Markov since 1981. A few prototype modules for the deep underwater neutrino telescope NESTOR and the hydroacoustic neutrino telescope SADCO were designed, constructed and tested in the Mediterranean Sea in 1987—1992 [3]. Four expeditions to Antarctica in 1985—1990 had shown good possibilities for radiowave neutrino telescope RAMAND [4].

In this paper the prospects for the large-scale neutrino telescopes — acoustic and radiowave ones — are discussed. Such detectors could compliment the optical Cherenkov neutrino detectors to search for the neutrinos from the AGN or even from the topological defects. Some of the results were presented earlier at the Conferences EPS HEP-95 in Brussels and ICHEP-96 in Warsaw.

REFERENCES

1. **Markov M.A.** — Proc. 10th Int. Conf. High-Energy Physics, Rochester, 1960, p.579; **Markov M.A., Zheleznykh I.M.** — In: High-Energy Neutrino Physics, D-577, Dubna, 1960; **Markov M.A., Zheleznykh I.M.** — Nucl. Phys., 1961, v.27, p.385.
2. **Markov M.A., Zheleznykh I.M.** — NIM, 1986, v.A248, p.242.
3. **Butkevich A.V., Karaevsky S.K., Markov M.A. et al.** — Tubner-Texte für Physik, 1994, v.B28, p.128.
4. **Boldyrev I.N., Gusev G.A., Markov M.A. et al.** — Proc. 3rd Int. Workshop on Neutrino Telescopes, Ed. Milla Baldo Ceolin, Venezia, 1991, p.337.

I.Zheleznykh, Oct. 7, 1997.